

Copper(II) Complexes of Pyridyl-Appended Diazacycloalkanes: Synthesis, Characterization, and Application to Catalytic Olefin Aziridination

Jason A. Halfen,^{*,†} Joseph M. Uhan,[†] Derek C. Fox,[†] Mark P. Mehn,[‡] and Lawrence Que, Jr.[‡]

Department of Chemistry, University of Wisconsin—Eau Claire, 105 Garfield Avenue, Eau Claire, Wisconsin 54701, and Department of Chemistry and Center for Metals in Biocatalysis, The University of Minnesota, 207 Pleasant Street S.E., Minneapolis, Minnesota 55455

Received June 14, 2000

As part of an ongoing effort to rationally design new copper catalysts for olefin aziridination, a family of copper(II) complexes derived from new tetradentate macrocyclic ligands are synthesized, characterized both in the solid state and in solution, and screened for catalytic nitrene transfer reactivity with a representative set of olefins. The pyridylmethyl-appended diazacycloalkane ligands $L^6(\text{py})_2$, $L^7(\text{py})_2$, and $L^8(\text{py})_2$ are prepared by alkylation of the appropriate diazacycloalkane (piperazine, homopiperazine, or diazacyclooctane) with picolyl chloride in the presence of triethylamine. The ligands are metalated with $\text{Cu}(\text{ClO}_4)_2 \cdot 6\text{H}_2\text{O}$ to provide the complexes $[(L^6(\text{py})_2)\text{Cu}(\text{OCIO}_3)]\text{ClO}_4$ (**1**), $[(L^7(\text{py})_2)\text{Cu}(\text{OCIO}_3)]\text{ClO}_4$ (**2**), and $[(L^8(\text{py})_2)\text{Cu}](\text{ClO}_4)_2$ (**3**), which, after metathesis with NH_4PF_6 in CH_3CN , afford $[(L^6(\text{py})_2)\text{Cu}(\text{CH}_3\text{CN})](\text{PF}_6)_2$ (**4**), $[(L^7(\text{py})_2)\text{Cu}(\text{CH}_3\text{CN})](\text{PF}_6)_2$ (**5**), and $[(L^8(\text{py})_2)\text{Cu}](\text{PF}_6)_2$ (**6**). All six complexes are characterized by X-ray crystallography, which reveals that complexes supported by $L^6(\text{py})_2$ and $L^7(\text{py})_2$ (**1**, **2**, **4**, **5**) adopt square-pyramidal geometries, while complexes **3** and **6**, ligated by $L^8(\text{py})_2$, feature tetracoordinate, distorted-square-planar copper ions. Tetragonal geometries in solution and $d(x^2 - y^2)$ ground states are confirmed for the complexes by a combination of UV–visible and EPR spectroscopies. The divergent flexibility of the three supporting ligands influences the Cu(II)/Cu(I) redox potentials within the family, such that the complexes supported by the larger ligands $L^7(\text{py})_2$ and $L^8(\text{py})_2$ (**5** and **6**) exhibit quasi-reversible electron transfer processes ($E_{1/2} \sim -0.2$ V vs Ag/AgCl), while the complex supported by $L^6(\text{py})_2$ (**4**), which imposes a rigid tetragonal geometry upon the central copper(II) ion, is irreversibly reduced in CH_3CN solution. Complexes **4–6** are efficient catalysts (in 5 mol % amounts) for the aziridination of styrene with the iodine PhINTs (in 80–90% yields vs PhINTs), while only **4** exhibits significant catalytic nitrene transfer reactivity with 1-hexene and cyclooctene.

Introduction

The development of new catalytic methods for the preparation of aziridines remains an area of active investigation owing to the utility of the aziridine ring in organic synthesis,¹ as well as the potent cytotoxic properties of several aziridine-containing natural products.² Current catalytic routes to aziridines rely principally on group transfer processes, namely carbene addition to imines and nitrene transfer to olefins; such reactions are often mediated by transition metals (via coordination of the carbene/nitrene)³ or Lewis acids (via substrate activation).⁴ Both routes have been exploited in asymmetric applications.⁵ First reported by Evans in 1991,^{3a} copper-mediated nitrene transfer reactions from (tosylimino)phenyliodinane (PhINTs)⁶ to alkenes remain

among the most widely applied catalytic routes to *N*-tosylaziridines. The scope of this olefin aziridination reaction has been extended by investigation of catalysts derived from other metals (principally Rh)⁷ and by the application of alternative nitrene sources.⁸

We recently initiated a systematic investigation of the structural and electronic factors that regulate the catalytic activity of copper complexes in nitrene transfer reactions from PhINTs to olefins. Previously, we described the utility of a triazacyclonane-ligated copper complex, $[(i\text{-Pr}_3\text{TACN})\text{Cu}(\text{O}_2\text{CCF}_3)_2]$, in catalytic olefin aziridination, in that this catalyst need only be used in 0.5 mol % amounts relative to PhINTs to effect the near-quantitative aziridination of styrene derivatives.⁹ Herein we present the synthesis and characterization of a family of new

* Corresponding author. Phone: 715-836-4179. Fax: 715-836-4979. E-mail: halfenja@uwec.edu.

[†] University of Wisconsin—Eau Claire.

[‡] The University of Minnesota.

- (1) (a) Tanner, D. *Angew. Chem., Int. Ed. Engl.* **1994**, *35*, 599–619. (b) Pearson, W. H.; Lian, B. W.; Bergmeier, S. C. In *Comprehensive Heterocyclic Chemistry II*; Padwa, A., Ed.; Pergamon Press: Oxford, U.K., 1996; Vol. 1A, pp 1–60. (c) Rai, K. M. L.; Hassner, A. In *Comprehensive Heterocyclic Chemistry II*; Padwa, A., Ed.; Pergamon Press: Oxford, U.K., 1996; Vol. 1A, pp 61–96.
- (2) For example, consider Mitomycin C and Azinomycins A and B, recent syntheses of which are described respectively by: (a) Fukuyama, T.; Yang, L. *J. Am. Chem. Soc.* **1989**, *111*, 8303–8304. (b) Coleman, R. S.; Kong, J.-S. *J. Am. Chem. Soc.* **1998**, *120*, 3538–3539.

- (3) (a) Evans, D. A.; Faul, M. M.; Bilodeau, M. T. *J. Org. Chem.* **1991**, *56*, 6744–6746. (b) Perez, P. J.; Brookhart, M.; Templeton, J. L. *Organometallics* **1993**, *12*, 261–262. (c) Evans, D. A.; Faul, M. M.; Bilodeau, M. T. *J. Am. Chem. Soc.* **1994**, *116*, 2742–2753. (d) Hansen, K. B.; Finney, N. S.; Jacobsen, E. N. *Angew. Chem., Int. Ed. Engl.* **1995**, *34*, 676–678. (e) Dauban, P.; Dodd, R. H. *Tetrahedron Lett.* **1998**, *39*, 5739–5742.
- (4) (a) Rasmussen, K. G.; Jorgensen, K. A. *J. Chem. Soc., Chem. Commun.* **1995**, 1401–1402. (b) Zhu, Z.; Espenson, J. H. *J. Org. Chem.* **1995**, *60*, 7090–7091. (c) Casarrubois, L.; Perez, J. A.; Brookhart, M.; Templeton, J. L. *J. Org. Chem.* **1996**, *61*, 8358–8359. (d) Mayer, M. F.; Hossain, M. M. *J. Org. Chem.* **1998**, *63*, 6839–6844. (e) Juhl, K.; Hazell, R. G.; Jorgensen, K. A. *J. Chem. Soc., Perkin Trans. 1* **1999**, 2293–2297.

copper(II) complexes, supported by pyridyl-appended diazacycloalkane ligands, and the results of a preliminary examination of their ability to catalyze the aziridination of olefins. The solid-state structures of these six complexes were determined by X-ray crystallography, and their solution structures were probed by spectroscopic and electrochemical methods. All of the complexes examined were found to be active catalysts for the aziridination of styrene, and one complex also catalyzed the aziridination of aliphatic olefins.

Experimental Section

Materials and Methods. Solvents and reagents were obtained from commercial sources and used as received unless noted otherwise. Styrene was distilled from KOH pellets at 25 °C under vacuum (0.3 Torr) and was stored over molecular sieves at -20 °C. Anhydrous acetonitrile (Aldrich Sure-Seal) was used in catalytic aziridinations and was handled and stored under N₂. The iodine PhINTs was prepared by a modified literature procedure and was stored in the dark.⁶ The dihydrobromide salt of 1,5-diazacyclooctane was prepared as described in the literature.¹⁰ NMR spectra were obtained using a JEOL Eclipse 400 spectrometer at room temperature. ¹H and ¹³C{¹H} chemical shifts are reported vs TMS and are referenced to residual solvent peaks. FTIR spectra (4000–400 cm⁻¹ range) were recorded on a Nicolet 5DXC spectrometer for samples in the form of dispersions in KBr or as thin films between KBr plates. Electronic absorption spectra were acquired by using a Hewlett-Packard 8453 spectrophotometer (190–1100 nm range), and mass spectra were obtained with a Hewlett-Packard GC/MS system operating in the electron impact ionization mode. X-band EPR spectra were recorded on a Bruker E-500 spectrometer with sample temperatures maintained at 10 K with an Oxford Instruments EPR-10 liquid helium cryostat. Spectra were recorded using a time constant of 82 ms, a sweep time of 82 ms, a modulation amplitude of 3 G, a modulation frequency of 100 kHz, and a power of 0.02 mW to avoid saturation. EPR spectral parameters were deduced from simulations of the experimental spectra using the program WINEPR SimFonia. Electrochemical experiments were conducted with a BAS CV50 potentiostat, using a glassy carbon working electrode, an Ag/AgCl reference electrode, and a platinum wire auxiliary electrode. Cyclic voltammograms were obtained in CH₃CN (0.1 M *n*-Bu₄NClO₄) with analyte concentrations of 1 mM. Melting points were determined using a Fisher-Johns melting point apparatus in open capillaries and are uncorrected. Elemental analyses were performed by Galbraith Laboratories, Knoxville TN. *Caution!* Perchlorate salts of transition metal complexes containing organic ligands are potentially explosive and should be prepared in small quantities and handled with appropriate precautions. While no difficulties were encountered with the complexes reported herein, due caution should be exercised.

- (5) (a) Müller, P. In *Advances in Catalytic Processes*; Doyle, M. P., Ed.; JAI Press Inc.: Greenwich, CT, 1996; Vol. 2, pp 113–151. (b) Li, Z.; Conser, K. R.; Jacobsen, E. N. *J. Am. Chem. Soc.* **1993**, *115*, 5326–5327. (c) Evans, D. A.; Faul, M. M.; Bilodeau, M. T.; Anderson, B. A.; Barnes, D. M. *J. Am. Chem. Soc.* **1993**, *115*, 5328–5329. (d) Noda, K.; Hosoya, N.; Irie, R.; Ito, Y.; Katsuki, T. *Synlett* **1993**, 469–471. (e) Antilla, J. C.; Wulff, W. D. *J. Am. Chem. Soc.* **1999**, *121*, 5099–5100. (f) Lai, T.-S.; Kwong, H.-L.; Che, C.-M.; Peng, S.-M. *J. Chem. Soc., Chem. Commun.* **1997**, 2372–2374.
- (6) Yamada, Y.; Yamamoto, T.; Okawara, M. *Chem. Lett.* **1975**, 361–362.
- (7) (a) Müller, P.; Baud, C.; Jacquier, Y. *Can. J. Chem.* **1998**, *76*, 738–750. (b) Müller, P.; Baud, C.; Jacquier, Y.; Moran, M.; Nageli, I. *J. Phys. Org. Chem.* **1996**, *9*, 341–347.
- (8) (a) Sodergren, M. J.; Alonso, D. A.; Andersson, P. G. *Tetrahedron: Asymmetry* **1997**, *8*, 3563–3565. (b) Albone, D. P.; Aujla, P. S.; Taylor, P. C.; Challenger, S.; Derrick, A. M. *J. Org. Chem.* **1998**, *63*, 9569–9571. (c) Dauban, P.; Dodd, R. H. *J. Org. Chem.* **1999**, *64*, 5304–5307. (d) Mephrathu, B. V.; Diltz, S.; Walsh, P. J.; Protasiewicz, J. D. *Tetrahedron Lett.* **1999**, *40*, 5459–5460. (e) Gontcharov, A. V.; Liu, H.; Sharpless, K. B. *Org. Lett.* **1999**, *1*, 783–786.
- (9) Halfen, J. A.; Hallman, J. K.; Schultz, J. A.; Emerson, J. P. *Organometallics* **1999**, *18*, 5435–5437.
- (10) Houser, R. P.; Young, V. G., Jr.; Tolman, W. B. *J. Am. Chem. Soc.* **1996**, *118*, 2101–2102.

1,4-Bis(pyridin-2-ylmethyl)piperazine, L⁶(py)₂. A solution of piperazine (1.010 g, 11.73 mmol) in CH₃CN (40 mL) was treated with 2-picolyl chloride hydrochloride (3.943 g, 24.04 mmol) and triethylamine (6.5 mL), and the resultant mixture was stirred in a loosely sealed flask at room temperature. After 48 h, the heterogeneous mixture was poured into 1 M NaOH (100 mL) and extracted with CH₂Cl₂ (3 × 50 mL). The combined extracts were dried (MgSO₄) and evaporated to yield the crude product as a brown solid. The solid was dissolved in diethyl ether (50 mL) and heated to reflux, resulting in the deposition of an insoluble brown oil. The ether solution was decanted from the oil and then treated with activated carbon, heated briefly, and filtered. The ether solution was evaporated to yield the pure product as a colorless crystalline solid: yield 1.673 g (53%); mp 93–96 °C; ¹H NMR (CDCl₃, 400 MHz) δ 8.55 (m, 2H), 7.64 (m, 2H), 7.39 (br d, 2H), 7.15 (m, 2H), 3.67 (s, 4H), 2.57 (br s, 8H) ppm; ¹³C{¹H} NMR (CDCl₃, 100 MHz) δ 158.4, 149.1, 136.2, 123.1, 121.8, 64.5, 53.1 ppm; FTIR (KBr) 3055, 3012, 2969, 2944, 2802, 2753, 1586, 1567, 1431, 1345, 1308, 1166, 1129, 1017, 845, 758, 727, 604, 468 cm⁻¹; LREIMS *m/z* 268 (M⁺). Anal. Calcd for C₁₆H₂₀N₄: C, 71.61; H, 7.51; N, 20.88. Found: C, 71.15; H, 7.48; N, 20.53.

1,4-Bis(pyridin-2-ylmethyl)-1,4-diazepane, L⁷(py)₂. In a procedure similar to that used to prepare L⁶(py)₂, a mixture of homopiperazine (1.030 g, 10.30 mmol), 2-picolyl chloride hydrochloride (3.313 g, 20.20 mmol), triethylamine (5.7 mL), and CH₃CN (45 mL) was stirred in a loosely sealed flask for 48 h. Following treatment of the mixture with aqueous NaOH and extraction into CH₂Cl₂, the crude ligand was isolated as a dark brown oil. Purification by Kugelrohr distillation (150 °C, 0.5 Torr) afforded the pure product as a light yellow oil: yield 1.866 g (64%); ¹H NMR (CDCl₃, 400 MHz) δ 8.43 (m, 2H), 7.54 (m, 2H), 7.37 (br d, 2H), 7.03 (m, 2H), 3.72 (s, 4H), 2.71 (t, *J* = 5.8 Hz, 4H), 2.67 (s, 4H), 1.74 (pentet, *J* = 5.9 Hz, 2H) ppm; ¹³C{¹H} NMR (CDCl₃, 100 MHz) δ 159.9, 149.0, 136.4, 122.9, 121.8, 64.3, 55.4, 54.7, 27.7 ppm; FTIR (neat) 3061, 3006, 2944, 2821, 1586, 1481, 1431, 1357, 1246, 1122, 1042, 993, 764, 616 cm⁻¹; LREIMS *m/z* 282 (M⁺). Anal. Calcd for C₁₇H₂₂N₄·0.5H₂O: C, 70.07; H, 7.96; N, 19.23. Found: C, 70.42; H, 7.88; N, 19.38.

1,5-Bis(pyridin-2-ylmethyl)-1,5-diazocane, L⁸(py)₂. The reaction was conducted as described above for L⁶(py)₂, using 1,5-diazacyclooctane dihydrobromide (2.327 g, 8.43 mmol), 2-picolyl chloride hydrochloride (2.760 g, 16.83 mmol), and triethylamine (6.5 mL) in CH₃CN (50 mL). The crude product, a dark oil, was treated with hot hexane (150 mL) and gravity-filtered to remove insoluble material, and the filtrate was evaporated to yield a light yellow oil that crystallized on standing. This solid was recrystallized from boiling hexane in the presence of activated charcoal to provide the pure product as a colorless crystalline solid: yield 1.467 g (59%); mp 50–53 °C; ¹H NMR (CDCl₃, 400 MHz) δ 8.49 (m, 2H), 7.61 (m, 2H), 7.46 (m, 2H), 7.10 (m, 2H), 3.81 (s, 4H), 2.79 (t, *J* = 5.9 Hz, 8H), 1.65 (pentet, *J* = 5.9 Hz, 4H) ppm; ¹³C{¹H} NMR (CDCl₃, 100 MHz) δ 160.7, 149.0, 136.4, 123.0, 121.8, 63.4, 53.0, 26.8 ppm; FTIR (KBr) 3080, 3049, 3012, 2963, 2901, 2802, 1586, 1567, 1468, 1437, 1357, 1178, 1160, 1079, 999, 894, 764, 622 cm⁻¹; LREIMS *m/z* 296 (M⁺). Anal. Calcd for C₁₈H₂₄N₄: C, 72.94; H, 8.16; N, 18.90. Found: C, 72.14; H, 8.13; N, 18.71.

[(L⁶(py)₂)Cu(OClO₃)]ClO₄, 1. A solution of L⁶(py)₂ (0.101 g, 0.375 mmol) in CH₃CN (15 mL) was treated with [Cu(H₂O)₆](ClO₄)₂ (0.139 g, 0.376 mmol), causing a deep blue color to develop. After 15 min of stirring, diethyl ether was allowed to diffuse into the solution over a period of several days, resulting in the deposition of blue crystals of the product: yield 0.164 g (82%); FTIR (KBr) 3018, 2907, 1715, 1444, 1380, 1221, 1132, 1092, 628, 542 cm⁻¹; UV-vis (CH₃CN) [λ_{max}, nm (ε, M⁻¹ cm⁻¹)] 262 (11 500), 286 (sh, 3800), 645 (310). Anal. Calcd for C₁₆H₂₀N₄Cl₂CuO₈: C, 36.20; H, 3.80; N, 10.56. Found: C, 37.03; H, 4.02; N, 11.16.

[(L⁷(py)₂)Cu(OClO₃)]ClO₄, 2. A procedure analogous to that used to prepare 1 was followed, substituting L⁷(py)₂ (0.118 g, 0.419 mmol). The pure product was isolated as dark blue crystals: yield 0.185 g (81%); FTIR (KBr) 3105, 3074, 2956, 2926, 2876, 1610, 1487, 1462, 1431, 1160, 1129, 1104, 1042, 770, 622 cm⁻¹; UV-vis (CH₃CN) [λ_{max}, nm (ε, M⁻¹ cm⁻¹)] 261 (11 400), 283 (sh, 4500), 621 (320). Anal. Calcd for C₁₇H₂₂N₄Cl₂CuO₈: C, 37.48; H, 4.07; N, 10.28. Found: C, 37.23; H, 4.19; N, 10.08.

[(L⁸(py)₂)Cu](ClO₄)₂, 3. A procedure analogous to that used to prepare **1** was followed, substituting L⁸(py)₂ (0.112 g, 0.376 mmol). The pure product was isolated as dark violet crystals: yield 0.128 g (61%); FTIR (KBr) 3092, 3043, 2932, 2870, 1610, 1487, 1462, 1445, 1122, 1098, 1067, 1030, 993, 777, 622 cm⁻¹; UV-vis (CH₃CN) [λ_{max} , nm (ϵ , M⁻¹ cm⁻¹)] 261 (11 600), 290 (sh, 4100), 602 (290). Anal. Calcd for C₁₈H₂₄N₄Cl₂CuO₈: C, 38.68; H, 4.33; N, 10.03. Found: C, 38.64; H, 4.46; N, 9.90.

[(L⁶(py)₂)Cu(CH₃CN)](PF₆)₂, 4. A solution containing L⁶(py)₂ (0.105 g, 0.392 mmol) and [Cu(H₂O)₆](ClO₄)₂ (0.145 g, 0.390 mmol) in CH₃CN (10 mL) was treated with a suspension of NH₄PF₆ (1.278 g, 7.840 mmol, 20.1 equiv) in CH₃OH (10 mL). The resulting mixture was stored at -20 °C for several hours and then filtered. The crude solid product was treated with CH₃CN (20 mL), the mixture was filtered to remove excess NH₄PF₆, and the filtrate was slowly evaporated to provide the product as blue crystals: yield 0.190 g (73%); FTIR (KBr) 3092, 3000, 2944, 2901, 2320, 2290 (C≡N), 1616, 1499, 1460, 1376, 1318, 1195, 1098, 851 (PF₆⁻), 783, 573 cm⁻¹; UV-vis (CH₃CN) [λ_{max} , nm (ϵ , M⁻¹ cm⁻¹)] 261 (7900), 641 (320). Anal. Calcd for C₁₈H₂₃N₅-CuF₁₂P₂·H₂O: C, 31.75; H, 3.70; N, 10.29. Found: C, 31.41; H, 3.62; N, 9.96.

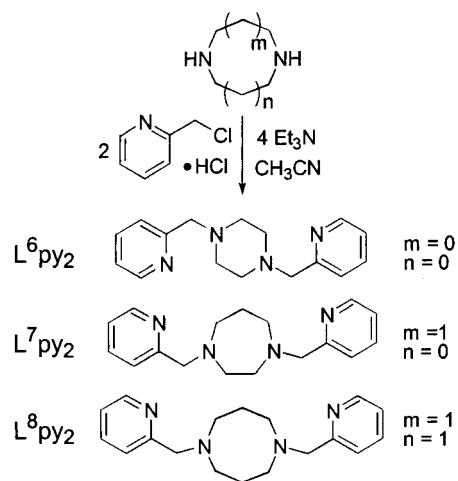
[(L⁷(py)₂)Cu(CH₃CN)](PF₆)₂, 5. A procedure analogous to that used to prepare **4** was followed, substituting L⁷(py)₂ (0.116 g, 0.412 mmol). The pure product was isolated as blue crystals: yield 0.133 g (45%); FTIR (KBr) 3105, 2987, 2913, 2870, 2314, 2277 (C≡N), 1620, 1487, 1462, 1314, 1104, 1048, 851 (PF₆⁻), 783, 567 cm⁻¹; UV-vis (CH₃CN) [λ_{max} , nm (ϵ , M⁻¹ cm⁻¹)] 261 (16 700), 623 (280). Anal. Calcd for C₁₉H₂₅N₅CuF₁₂P₂: C, 33.71; H, 3.72; N, 10.35. Found: C, 33.94; H, 3.92; N, 10.35.

[(L⁸(py)₂)Cu](PF₆)₂, 6. A procedure analogous to that used to prepare **4** was followed, substituting L⁸(py)₂ (0.116 g, 0.412 mmol). The crude product was isolated by adding H₂O (10 mL) to the reaction mixture, followed by cooling to -20 °C. Recrystallization from hot CH₃OH followed by slow cooling to -20 °C provided violet crystals: yield 0.145 g (54%); FTIR (KBr) 3098, 2981, 2876, 1616, 1444, 1308, 1122, 993, 838 (PF₆⁻), 554 cm⁻¹; UV-vis (CH₃CN) [λ_{max} , nm (ϵ , M⁻¹ cm⁻¹)] 261 (12 000), 300 (sh, 3800), 601 (260); UV-vis (CH₃OH) [λ_{max} , nm (ϵ , M⁻¹ cm⁻¹)] 599 (240). Anal. Calcd for C₁₈H₂₄N₄CuF₁₂P₂: C, 33.27; H, 3.72; N, 8.62. Found: C, 33.43; H, 3.90; N, 8.67.

Catalytic Aziridinations: Styrene. Aziridinations were performed by stirring mixtures of PhINTs (0.3–0.4 mmol), styrene (1.0 mL), and the copper catalyst (5 mol % vs PhINTs) in 2 mL of anhydrous CH₃CN under a dry N₂ atmosphere as described previously. At the completion of the reactions, the clear, purple solutions were passed through a short column of neutral alumina to remove copper species, eluted with EtOAc, and the eluates were evaporated to yield oily residues. These crude product mixtures (of iodobenzene, 2-phenyl-1-tosylaziridine, and *p*-toluenesulfonamide) were treated with hexane to produce the crude aziridine products, which were recrystallized from hexane/Et₂O mixtures at -20 °C. Data for 2-phenyl-1-tosylaziridine: mp 88–90 °C (lit.^{3c} 88–89 °C); ¹H NMR (CDCl₃, 400 MHz) δ 7.86 (d, 2H), 7.32 (d, 2H), 7.31–7.21 (m, 5H), 3.77 (dd, 1H), 2.97 (d, 1H), 2.42 (s, 3H), 2.38 (d, 1H) ppm; ¹³C{¹H} NMR (CDCl₃, 100 MHz) δ 144.8, 135.1, 135.0, 129.9, 128.7, 128.4, 128.0, 126.6, 41.1, 36.0, 21.8 ppm; LREIMS *m/z* 273 (M⁺).

Catalytic Aziridinations: 1-Hexene and Cyclooctene. Aziridinations were performed as described above by stirring mixtures of PhINTs (0.3–0.4 mmol), the olefin (1.0 mL), and the copper catalyst (5 mol % vs PhINTs) in 2 mL of anhydrous CH₃CN. At the completion of the reactions, the clear, purple solutions were passed through a short column of neutral alumina to remove copper species, eluted with EtOAc, and the eluates were evaporated to yield semisolid residues. These crude product mixtures were treated with hexane, and the resultant mixtures were filtered to remove *p*-toluenesulfonamide. The filtrates were evaporated and dried overnight under vacuum to yield the pure aziridine products. Data for 2-butyl-1-tosylaziridine: bp 120 °C (0.3 Torr); ¹H NMR (CDCl₃, 400 MHz) δ 7.81 (d, 2H), 7.32 (d, 2H), 7.31–7.21 (m, 5H), 2.70 (m, 1H), 2.62 (d, 1H), 2.43 (s, 3H), 2.04 (d, 1H), 1.52 (m, 1H), 1.38–1.18 (m, 5H), 0.80 (t, 3H) ppm; ¹³C{¹H} NMR (CDCl₃, 100 MHz) δ 144.5, 135.2, 129.7, 40.5, 33.9, 31.1, 31.0, 28.9, 22.2, 21.7, 13.9 ppm; LREIMS *m/z* 254 (M⁺). Data for 9-tosyl-9-azabicyclo-

Scheme 1



[6.1.0]nonane: mp 122 °C; ¹H NMR (CDCl₃, 400 MHz) δ 7.80 (d, 2H), 7.31 (d, 2H), 2.76 (dd, 1H), 2.43 (s, 3H), 2.00 (dd, 1H), 1.56–1.24 (m, 12H) ppm; ¹³C{¹H} NMR (CDCl₃, 100 MHz) δ 144.2, 135.9, 129.7, 127.7, 44.0, 29.8, 26.5, 26.3, 25.3, 21.7 ppm; LREIMS *m/z* 279 (M⁺).

X-ray Crystallography. Single crystals of the compounds were mounted in thin-walled glass capillaries and transferred to the goniometer of an Enraf-Nonius CAD4 X-ray diffractometer for data collections at 25 °C using graphite-monochromated Mo K α (λ = 0.710 73 Å) radiation. Unit cell constants were determined from a least-squares refinement of the setting angles of 25 machine-centered intense, high-angle reflections. Intensity data were collected using the $\omega/2\theta$ scan technique to a maximum 2θ value of 50–52°. Absorption corrections based on azimuthal scans of several reflections for each sample were applied. The data were corrected for Lorentz and polarization effects and converted to structure factors using the teXsan for Windows crystallographic software package.¹¹ Space groups were determined on the basis of systematic absences and intensity statistics. A successful direct-methods solution was calculated for each compound using the SHELXTL suite of programs.¹² Any non-hydrogen atoms not identified from the initial *E* map were located after several cycles of structure expansion and full-matrix least-squares refinement. Hydrogen atoms were added geometrically. All non-hydrogen atoms were refined with anisotropic displacement parameters, while hydrogen atoms were refined using a riding model with group isotropic displacement parameters. Relevant crystallographic information for the compounds is summarized in Table 1, and selected interatomic distances and angles are provided in Table 2. Complete crystallographic data for each compound are provided as Supporting Information in CIF format.

The asymmetric unit of [(L⁶(py)₂)Cu(OCIO₃)]ClO₄ (**1**) contains two crystallographically unique yet chemically similar formula units. The ClO₄⁻ ions exhibit significant thermal motion, and nine geometric constraints were applied to one of these ions. In [(L⁷(py)₂)Cu(OCIO₃)]ClO₄ (**2**), the uncoordinated ClO₄⁻ ion is rotationally disordered and was refined using a split-atom model. Bond length constraints were applied to the two disordered groups, and neighboring oxygen atoms were constrained to have the same *U*_{ij} components. The structure of [(L⁸(py)₂)Cu](ClO₄)₂ (**3**) was well-behaved. The asymmetric unit of [(L⁶(py)₂)Cu(CH₃CN)](PF₆)₂ (**4**) contains half of the cation and two half-anions; each of these ions resides on a crystallographic mirror plane. In addition, the PF₆⁻ ion that is proximal to the copper center is disordered and was refined using a split-atom model. Many of the atoms in the structure of [(L⁷(py)₂)Cu(CH₃CN)](PF₆)₂ (**5**) exhibit high anisotropic displacement parameters, perhaps reflecting positional disorder that could not be resolved using data collected at room temperature. Consequently, the residuals for the model of **5** presented

(11) *teXsan for Windows*, Version 1.02; Molecular Structure Corp.: The Woodlands, TX, 1997–1998.

(12) *SHELXTL*, Version 5.1 for Windows NT; Bruker AXS: Madison, WI, 1998.

Table 1. Summary of X-ray Crystallographic Data^a

	1	2	3	4	5	6
empirical formula	C ₁₆ H ₂₀ Cl ₂ CuN ₄ O ₈	C ₁₇ H ₂₂ Cl ₂ CuN ₄ O ₈	C ₁₈ H ₂₄ Cl ₂ CuN ₄ O ₈	C ₁₈ H ₂₅ CuF ₁₂ N ₄ P ₂	C ₁₉ H ₂₅ CuF ₁₂ N ₄ P ₂	C ₁₈ H ₂₄ CuF ₁₂ N ₄ P ₂
fw	530.80	544.83	558.85	662.89	676.92	649.89
crystal system	monoclinic	triclinic	orthorhombic	orthorhombic	monoclinic	monoclinic
space group	<i>P2₁/n</i>	<i>P1</i>	<i>Pbca</i>	<i>Pbcm</i>	<i>P2₁/c</i>	<i>P2₁/c</i>
<i>a</i> (Å)	14.684(3)	8.498(1)	14.143(3)	11.312(1)	11.733(2)	14.416(4)
<i>b</i> (Å)	16.325(7)	9.079(1)	17.302(2)	13.545(4)	13.645(3)	15.284(1)
<i>c</i> (Å)	17.785(4)	14.944(3)	17.970(2)	16.615(3)	16.509(3)	11.161(2)
α (deg)	90	85.98(2)	90	90	90	90
β (deg)	108.77(2)	88.29(2)	90	90	91.01(3)	99.09(3)
γ (deg)	90	66.83(1)	90	90	90	90
<i>V</i> (Å ³)	4037(2)	1057.4(3)	4397(1)	2545.8(9)	2642.6(9)	2428.3(8)
<i>Z</i>	8	2	8	4	4	4
d_{calcd} (Mg m ⁻³)	1.747	1.711	1.688	1.730	1.701	1.778
crystal size (mm)	0.42 × 0.35 × 0.30	0.48 × 0.25 × 0.25	0.50 × 0.38 × 0.08	0.50 × 0.50 × 0.35	0.50 × 0.50 × 0.45	0.50 × 0.30 × 0.30
abs coeff (mm ⁻¹)	1.401	1.340	1.291	1.090	1.052	1.140
2 θ max (deg)	51.88	51.94	49.88	51.92	51.88	51.88
no. of reflns collected	8168	4432	3836	2579	5421	4989
no. of independent reflns	7854	4134	3836	2579	5162	4734
<i>R</i> (int)	0.0598	0.0227	0	0	0.0349	0.0427
transm range	1.0–0.8285	1.0–0.9134	1.0–0.7882	1.0–0.8668	1.0–0.7885	1.0–0.8892
no. of obsd reflns	4384	2974	2234	1483	2524	2636
no. of variable parameters	559	317	298	214	352	334
<i>R1</i> (w <i>R2</i>) ^b [<i>I</i> > 2 σ (<i>I</i>)]	0.0698 (0.1674)	0.0508 (0.1235)	0.0635 (0.1502)	0.0540 (0.1258)	0.0889 (0.2287)	0.0521 (0.1129)
goodness-of-fit (<i>F</i> ²)	1.030	1.017	0.988	1.008	1.046	1.007
difference peaks (e Å ⁻³)	0.938, -0.717	0.801, -0.588	0.619, -1.063	0.401, -0.434	1.017, -0.613	0.518, -0.341

^a See Experimental Section for additional data collection and reduction and structure solution and refinement details. ^b $R1 = \sum ||F_o| - |F_c|| / \sum |F_o|$; $wR2 = [\sum (w(F_o^2 - F_c^2)^2)]^{1/2}$ where $w = 1/\sigma^2(F_o^2) + (aP)^2 + bP$.

herein are slightly higher than those reported for the other five structures. Finally, the structure of [(L⁸(py)₂)Cu](PF₆)₂ (**6**) was well-behaved.

Results and Discussion

Catalyst Designs and Syntheses. The ligands L⁶(py)₂, L⁷(py)₂, and L⁸(py)₂ (Scheme 1) were targeted because we speculated that these tetradentate ligands would occupy the four equatorial coordination positions in a square-planar or square-pyramidal copper(II) complex, leaving the axial coordination site(s) either vacant or occupied by a readily displaced solvent or counterion ligand. We reasoned that such an arrangement would facilitate the reaction of the copper(II) complexes derived from these ligands with the nitrene source PhINTs, as dissociation of one or more strongly donating ligands would not be required prior to the formation of the putative copper–nitrene intermediate.¹³ These tetradentate ligands were prepared by stirring mixtures of the appropriate diazacycloalkane (piperazine, homopiperazine, diazacyclooctane), picolyl chloride (2 equiv), and triethylamine (4 equiv) in CH₃CN solvent at room temperature for 24–48 h. Ligand syntheses conducted at reflux yielded irreproducible results, due in part to the high vapor pressures of the cyclic diamines at elevated temperatures, resulting in their loss from the reaction mixture. The ligands were isolated in good yields (50–70%) after purification by recrystallization or high-vacuum distillation; L⁶(py)₂ and L⁸(py)₂ are colorless to light yellow crystalline solids while L⁷(py)₂ is a light yellow oil that darkens upon prolonged exposure to the atmosphere.¹⁴ These chelates were characterized by spectroscopic and analytical methods and, in the case of L⁶(py)₂, by X-ray crystallography.¹⁵

Initial attempts to metalate L⁶(py)₂ involved the reaction of the ligand with CuCl₂·2H₂O and NH₄PF₆ in mixed CH₃OH/CH₃CN solvent, conditions that produced blue crystals of the cocrystallized mixture [(L⁶(py)₂)CuCl][(L⁶(py)₂)Cu₂(μ-Cl)](PF₆)₄ in modest yield, rather than the expected [(L⁶(py)₂)CuCl]PF₆ product.¹⁶ To avoid formation of this chloride-bridged dinuclear species, further metalations of the ligands were performed using Cu(ClO₄)₂·6H₂O, the ClO₄⁻ ions being exchanged with nonhazardous PF₆⁻ ions in a subsequent synthetic manipulation (Scheme 2). Thus, the reactions of L⁶(py)₂ and L⁷(py)₂ with Cu(ClO₄)₂·6H₂O in CH₃CN provided blue crystals of [LCu(OCIO₃)]ClO₄ (L = L⁶(py)₂ (**1**), L⁷(py)₂ (**2**)) in good yields. The presence of coordinated ClO₄⁻ ions in these complexes was inferred from infrared spectroscopic analysis (vide infra) and was confirmed for both by X-ray crystallography. In contrast, the parallel reaction of L⁸(py)₂ with Cu(ClO₄)₂·6H₂O in CH₃CN provided violet crystals of [(L⁸(py)₂)Cu](ClO₄)₂ (**3**), which lacks coordinated ClO₄⁻ ions, perhaps due to unfavorable steric interactions of the dual propylene groups in the diazacyclooctane backbone with potential axial ligands. Metathesis of the ClO₄⁻ ions in these complexes was accomplished by using an excess of NH₄PF₆ in mixed CH₃OH/CH₃CN solvent. Thus, the reaction of the above salts with NH₄PF₆ yielded blue solids that, after recrystallization from CH₃CN/Et₂O, provided blue crystals of [LCu(CH₃CN)](PF₆)₂ (L⁶(py)₂ (**4**), L⁷(py)₂ (**5**)) in which one axial coordination site of

(15) X-ray crystallographic data for L⁶(py)₂, C₁₆H₂₀N₄: Monoclinic, *P2₁/c*, with *a* = 5.796(1) Å, *b* = 7.372(2) Å, *c* = 17.335(4) Å, β = 98.84(3)°, *V* = 731.9(3) Å³, and *Z* = 2 at 25 °C. Full-matrix least-squares refinement based on *F*² provided current residuals of *R1* = 0.0497 and *wR2* = 0.1194 with GOF = 1.014 for 841 reflections with *I* > 2 σ (*I*) and 92 variables. Full details of the structure determination will be reported elsewhere.

(16) X-ray crystallographic data for [(L⁶(py)₂)CuCl][(L⁶(py)₂)Cu₂(μ-Cl)](PF₆)₄, C₄₈H₆₀Cl₂Cu₃F₂₄N₁₂P₄: triclinic, *P1*, with *a* = 13.090(3) Å, *b* = 13.736(2) Å, *c* = 18.388(3) Å, α = 77.43(1)°, β = 75.41(2)°, γ = 89.72(1)°, *V* = 3119(1) Å³, and *Z* = 2 at 25 °C. Full-matrix least-squares refinement based on *F*² provided current residuals of *R1* = 0.0631 and *wR2* = 0.1428 with GOF = 1.002 for 5943 reflections with *I* > 2 σ (*I*) and 838 variables. Full details of the structure determination will be reported elsewhere.

(13) (a) Li, Z.; Quan, R. W.; Jacobsen, E. N. *J. Am. Chem. Soc.* **1995**, *117*, 5889–5890. (b) Diaz Requejo, M. M.; Perez, P. J.; Brookhart, M.; Templeton, J. L. *Organometallics* **1997**, *16*, 4399–4402.

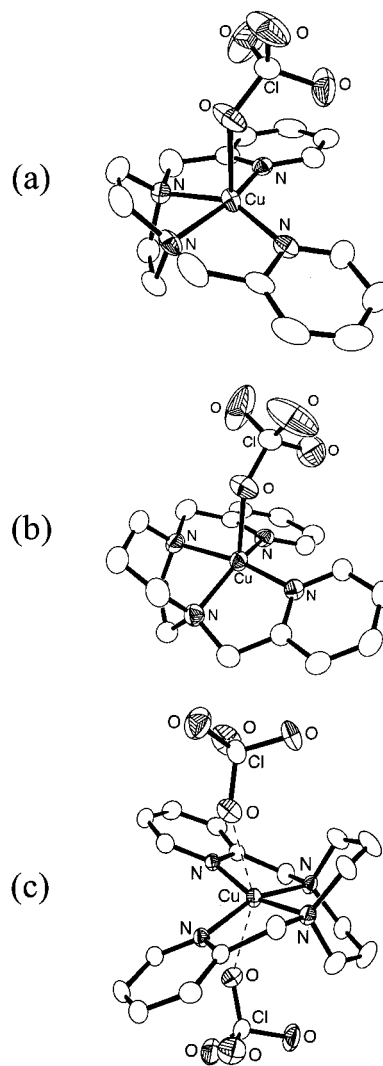
(14) The catalytic alkane hydroxylation reactivity of an Fe(II) complex of L⁷(py)₂, as well as an independent synthesis of the ligand, has been reported: Chen, K.; Que, L., Jr. *Angew. Chem., Int. Ed. Engl.* **1999**, *38*, 2227–2229.

Table 2. Selected Interatomic Distances (Å) and Angles (deg) for the Structurally Characterized Copper Complexes^a

Complex 1 ^b			
Cu(1)–N(1)	2.010(6)	N(2)–Cu(1)–N(1)	73.5(3)
Cu(1)–N(2)	2.000(6)	N(3)–Cu(1)–O(1)	98.3(2)
Cu(1)–N(3)	1.975(6)	N(4)–Cu(1)–O(1)	95.9(3)
Cu(1)–N(4)	1.993(6)	N(2)–Cu(1)–O(1)	93.1(2)
Cu(1)–O(1)	2.341(6)	N(1)–Cu(1)–O(1)	102.0(2)
Cu(1)···O(5)	3.246(9)	O(1)–Cu(1)···O(5)	163.7(3)
Cu(1a)–N(1a)	1.983(6)	N(4a)–Cu(1a)–N(1a)	159.3(2)
Cu(1a)–N(2a)	2.008(5)	N(4a)–Cu(1a)–N(3a)	115.1(2)
Cu(1a)–N(3a)	2.005(5)	N(4a)–Cu(1a)–N(2a)	85.0(2)
Cu(1a)–N(4a)	1.959(5)	N(1a)–Cu(1a)–N(3a)	82.5(2)
Cu(1a)–O(4a)	2.352(5)	N(1a)–Cu(1a)–N(2a)	74.5(2)
Cu(1a)···O(5a)	3.402(9)	N(3a)–Cu(1a)–N(2a)	147.0(2)
N(3)–Cu(1)–N(4)	115.4(2)	N(4a)–Cu(1a)–O(4a)	94.3(3)
N(3)–Cu(1)–N(2)	156.6(3)	N(1a)–Cu(1a)–O(4a)	93.8(3)
N(4)–Cu(1)–N(2)	83.4(2)	N(3a)–Cu(1a)–O(4a)	97.7(2)
N(3)–Cu(1)–N(1)	84.2(2)	N(2a)–Cu(1a)–O(4a)	107.0(2)
N(4)–Cu(1)–N(1)	151.3(2)	O(4a)–Cu(1a)···O(5a)	148.2(3)
Complex 2			
Cu(1)–N(1)	2.006(4)	N(3)–Cu(1)–N(1)	85.8(2)
Cu(1)–N(2)	2.003(4)	N(4)–Cu(1)–N(1)	143.4(2)
Cu(1)–N(3)	1.966(3)	N(2)–Cu(1)–N(1)	80.0(2)
Cu(1)–N(4)	2.002(4)	N(3)–Cu(1)–O(1)	87.4(2)
Cu(1)–O(1)	2.328(4)	N(4)–Cu(1)–O(1)	101.2(2)
N(3)–Cu(1)–N(4)	110.5(2)	N(2)–Cu(1)–O(1)	93.4(2)
N(3)–Cu(1)–N(2)	165.0(2)	N(1)–Cu(1)–O(1)	112.4(2)
N(4)–Cu(1)–N(2)	84.1(2)		
Complex 3			
Cu(1)–N(1)	2.001(5)	N(4)–Cu(1)–N(2)	85.5(2)
Cu(1)–N(2)	2.000(5)	N(3)–Cu(1)–N(2)	159.7(2)
Cu(1)–N(3)	1.975(5)	N(4)–Cu(1)–N(1)	163.0(2)
Cu(1)–N(4)	1.961(5)	N(3)–Cu(1)–N(1)	85.5(2)
Cu(1)···O(1)	2.827(5)	N(2)–Cu(1)–N(1)	89.6(2)
Cu(1)···O(5)	2.687(5)	O(1)···Cu(1)···O(5)	154.9(2)
N(4)–Cu(1)–N(3)	104.3(2)		
Complex 4 ^c			
Cu(1)–N(1)	2.013(4)	N(1)–Cu(1)–N(2a)	150.4(6)
Cu(1)–N(2)	2.015(4)	N(2)–Cu(1)–N(2a)	113.4(2)
Cu(1)–N(3)	2.172(6)	N(1)–Cu(1)–N(3)	103.5(2)
Cu(1)···F(4)	3.22(1)	N(2)–Cu(1)–N(3)	98.6(1)
N(1)–Cu(1)–N(1a)	73.5(3)	C(9)–N(3)–Cu(1)	155.5(7)
N(1)–Cu(1)–N(2)	82.5(2)	N(3)–Cu(1)···F(4)	150.3(3)
Complex 5			
Cu(1)–N(1)	1.967(8)	N(1)–Cu(1)–N(2)	154.5(4)
Cu(1)–N(2)	2.006(7)	N(4)–Cu(1)–N(2)	83.1(4)
Cu(1)–N(3)	1.994(8)	N(3)–Cu(1)–N(2)	110.6(3)
Cu(1)–N(4)	1.991(9)	N(1)–Cu(1)–N(1a)	102.9(4)
Cu(1)–N(1a)	2.237(9)	N(2)–Cu(1)–N(1a)	95.8(3)
N(1)–Cu(1)–N(4)	77.9(5)	N(3)–Cu(1)–N(1a)	95.0(3)
N(1)–Cu(1)–N(3)	85.0(4)	N(4)–Cu(1)–N(1a)	96.3(3)
N(4)–Cu(1)–N(3)	161.2(4)	C(1a)–N(1a)–Cu(1)	153.2(8)
Complex 6			
Cu(1)–N(1)	2.005(4)	N(4)–Cu(1)–N(2)	85.5(2)
Cu(1)–N(2)	1.998(4)	N(3)–Cu(1)–N(2)	158.2(2)
Cu(1)–N(3)	1.966(4)	N(4)–Cu(1)–N(1)	157.1(2)
Cu(1)–N(4)	1.962(4)	N(3)–Cu(1)–N(1)	84.6(2)
Cu(1)···F(1)	3.013(4)	N(2)–Cu(1)–N(1)	90.6(2)
Cu(1)···F(7)	2.925(4)	F(1)···Cu(1)···F(7)	136.1(1)
N(4)–Cu(1)–N(3)	106.8(2)		

^a Estimated standard deviations are indicated in parentheses. ^b Two crystallographically independent formula units are present in the asymmetric unit. ^c Atoms labeled with an "a" are related to atoms not so labeled by a crystallographic mirror plane.

each central copper ion is occupied by an acetonitrile molecule. Again, in a departure from the behavior observed for the complexes supported by L⁶(py)₂ and L⁷(py)₂, the copper(II) complex derived from L⁸(py)₂ was obtained in a violet, unsolvated form, [(L⁸(py)₂)Cu](PF₆)₂ (**6**), by recrystallization of the initial blue methathesis product from boiling CH₃OH. All of the copper(II) complexes that were prepared as part of this study were characterized by a combination of analytical, spectroscopic, and X-ray crystallographic methods.

**Figure 1.** Thermal ellipsoid representations (35% probability boundaries) of the X-ray crystal structures of **1** (a), **2** (b), and **3** (c). Hydrogen atoms and noncoordinated counterions are omitted for clarity.

Structural Characterization. X-ray crystallographic data for the complexes are collected in Table 1, while significant interatomic distances and angles are compiled in Table 2. Full listings of positional and anisotropic displacement parameters, as well as complete tables of interatomic distances and angles, in CIF format are provided as Supporting Information.

Perchlorato complexes [(L⁶(py)₂)Cu(OCIO₃)]ClO₄ (**1**) and [(L⁷(py)₂)Cu(OCIO₃)]ClO₄ (**2**) are characterized by the presence of square-pyramidal copper(II) ions in which the tetradentate ligands define the equatorial plane of the metal and a monodentate ClO₄[−] ion occupies an axial coordination site (Figure 1a,b). While two crystallographically independent but chemically similar formula units are found in the asymmetric unit of monoclinic crystals of **1**, the present discussion focuses on only one. The central copper(II) ion in **1** is displaced from the equatorial plane of nitrogen donors toward the axial perchlorate ligand (0.25 Å); an additional weak axial interaction trans to the bound ClO₄[−] ligand is also present. Triclinic crystals of **2** (Figure 1b) are compositionally similar to those of **1**. The propylene linker in the homopiperazine backbone of L⁷(py)₂, however, has subtle structural impacts on the coordination sphere of the copper ion. Principally, a ruffling of the equatorial plane is observed in **2**, such that the mean deviation of each nitrogen atom from the equatorial plane (defined by N(1), N(2), N(3),

and N(4)) is 0.28 Å, while the equivalent deviation in **1** is 0.07 Å. Similar to the case of **1**, however, the copper(II) ion in **2** is ligated by one ClO₄⁻ ion in an axial site, is displaced from the equatorial plane of nitrogens by 0.28 Å toward the axial perchlorate, and exhibits an additional weak axial interaction with a second ClO₄⁻ ion. In contrast to the crystallographic analyses of **1** and **2**, analysis of orthorhombic crystals of **3** (Figure 1c) revealed a distorted-square-planar geometry for the central copper(II) ion, which exhibits only weak axial interactions with two ClO₄⁻ ions. Consistent with the lack of significant axial bonding, the copper ion in **3** is only minimally displaced from the equatorial plane (0.03 Å toward the proximal ClO₄⁻ ion). As in the structure of **2**, the equatorial plane of nitrogen donors in **3** exhibits significant ruffling, in that the mean deviation of each nitrogen atom from the equatorial plane is 0.29 Å. The Cu–N bond lengths in **3** also exhibit a slight asymmetry, such that the Cu–N_{amine} bonds [average 2.000(5) Å] are slightly longer than the Cu–N_{pyridine} bonds [average 1.966(5) Å]; this bond length asymmetry is absent or less pronounced in **1** and **2**.

Comparison of the intraligand N–Cu–N bond angles in **1–3** reveals an interesting trend resulting from the presence of three different diazacycloalkane rings in the backbones of the complexes. Specifically, the N_{amine}–Cu–N_{amine} angles increase smoothly through the series, from a very acute angle in **1** [73.5(2)°] to a nearly ideal angle in **3** [89.6(2)°]. In the same fashion, the N_{pyridine}–Cu–N_{pyridine} angles decrease from an open angle in **1** [115.4(2)°] to a less strained angle in **3** [104.3(2)°]. Thus, the ligand bearing the largest macrocyclic backbone, L⁸(py)₂, allows the formation of more ideal basal plane geometries (the average interligand angular deviation in the basal plane of **3** from 90° is 5.8°, compared to 13.6° in **1**) while at the same time providing sufficient steric hindrance to prevent the formation of significant axial interactions.

Metathesis of **1** and **2** with NH₄PF₆ followed by crystallization from CH₃CN/Et₂O provided blue crystals of **4** and **5**, respectively, each having the composition [LCu(CH₃CN)](PF₆)₂. The asymmetric unit of orthorhombic crystals of [(L⁶(py)₂)Cu(CH₃CN)](PF₆)₂ (**4**, Figure 2a) contains half of the mononuclear dication and two distinct half-occupancy PF₆⁻ ions. Similar to its precursor **1**, complex **4** exhibits a square-pyramidal copper ion geometry, its coordination sphere being composed of the tetradentate L⁶(py)₂ ligand and an axial CH₃CN molecule that coordinates to the metal ion in a bent fashion [Cu(1)–N(3)–C(9) = 155.4(7)°] via an axial bond shorter than that observed for the axial ClO₄⁻ ligand in **1**. A weak axial interaction is also present between the copper ion and a PF₆⁻ counterion trans to the CH₃CN ligand. Crystallographic analysis of monoclinic crystals of [(L⁷(py)₂)Cu(CH₃CN)](PF₆)₂ (**5**, Figure 2b) revealed a similar overall structural topology for the complex, including a bent, axial CH₃CN ligand and a weak axial interaction trans to this ligand with a disordered PF₆⁻ ion. The Cu–N_{MeCN} bond length in **5** is slightly elongated (by 0.06 Å) relative to that found in **4**. In addition, two significant differences exist between **5** and its perchlorate-ligated precursor **2**. Specifically, the axial CH₃CN ligand in **5** and the propylene linker of the homopiperazine backbone of L⁷(py)₂ reside on opposite sides of the equatorial plane (observed in independent structure solutions using data collected from three different crystals). This relative disposition of the axial solvento ligand and the propylene linker may contribute to the lack of significant ruffling of the equatorial plane in **5** (the mean deviation of each nitrogen atom from this plane is 0.07 Å), as it relieves any possible steric interaction between these two groups. Metathesis of [(L⁸(py)₂)Cu](ClO₄)₂

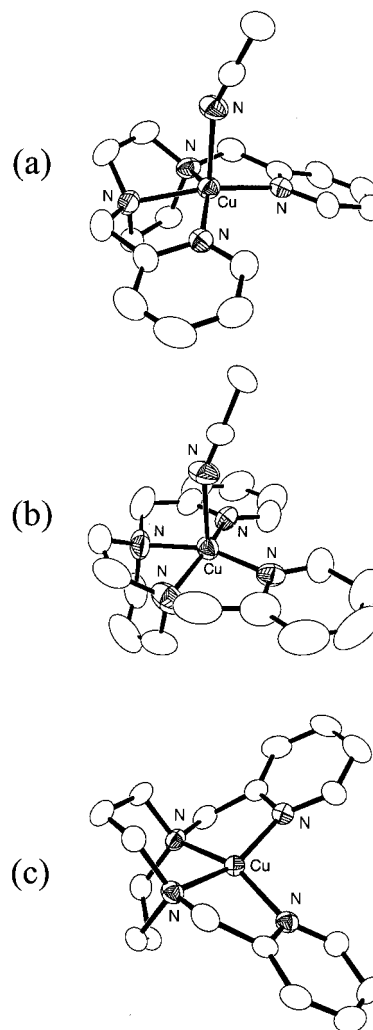
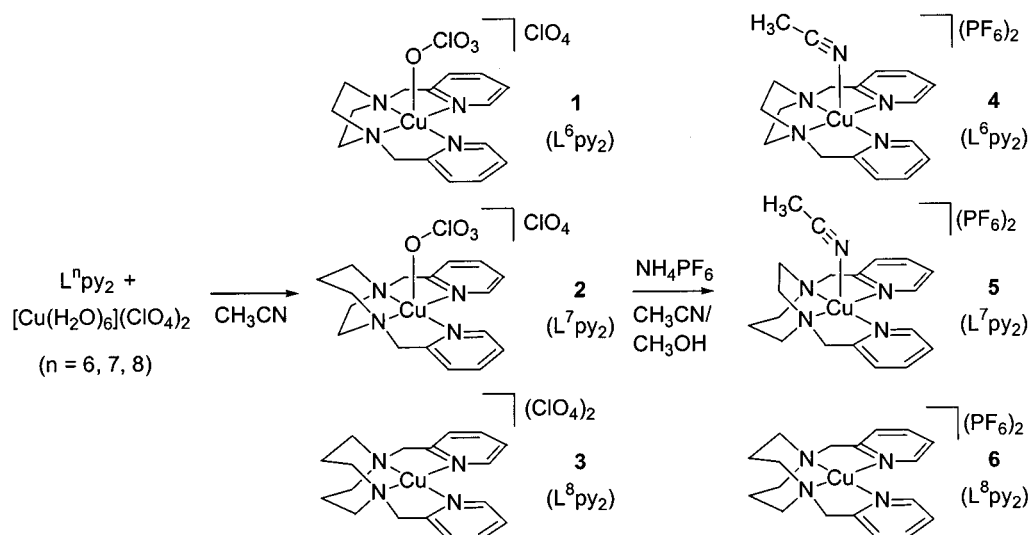


Figure 2. Thermal ellipsoid representations (35% probability boundaries) of the X-ray crystal structures of **4** (a), **5** (b), and **6** (c). Hydrogen atoms and counterions are omitted for clarity.

with NH₄PF₆ afforded well-formed violet crystals of solvent-free [(L⁸(py)₂)Cu](PF₆)₂ (**6**) that were amenable to crystallographic analysis. The X-ray crystal structure of **6** (Figure 2c) reveals a structural topology for the cation very similar to that observed in its ClO₄⁻ salt **3**, in that there are no significant axial bonding interactions between the central Cu(II) ion and the counterions, there is significant ruffling of the equatorial plane of nitrogen donors (the mean deviation of each nitrogen atom from this plane is 0.36 Å), and the metal ion is minimally displaced from this mean plane (0.01 Å). The six-membered chelate rings in **6** are conformationally distinct from those present in precursor **3** in that one of these two six-membered rings adopts a boat conformation in **6**, while both chelate rings adopt chair conformations in **3**.

Spectroscopic and Electrochemical Properties. The solid-state FTIR spectra of the copper complexes are consistent with their structures as determined by X-ray crystallography. Coordinated ClO₄⁻ ions in **1** and **2** are indicated by the presence of significant fine structure and splitting in the strong ClO₄⁻ vibrations observed near 1100 cm⁻¹. The axial CH₃CN ligands in **4** and **5** exhibit weak absorptions near 2280 cm⁻¹ that correspond to the C≡N stretch of the solvento ligands. In contrast, the FTIR spectrum of **6** lacks any vibrations attributable to a coordinated CH₃CN ligand, which is consistent with its tetracoordinate structure as defined by X-ray crystallography.

Scheme 2

Table 3. EPR Data for 1–3^a

complex	g_{\parallel} (A_{\parallel} (10^{-4} cm^{-1}))	g_{\perp}
1	2.21 (175)	2.05
2	2.21 (171)	2.05
3	2.20 (179)	2.05

^a Values quoted were obtained from simulations; see Experimental Section for data collection parameters. Experimental and simulated spectra are provided as Supporting Information.

Solutions of 1–3 in CH₃CN are indistinguishable by UV–visible spectroscopy from those of 4–6, respectively, suggesting a common solution structure for pairs of complexes supported by the same tetradentate ligand: square pyramidal with an axial CH₃CN ligand for complexes supported by L⁶(py)₂ and L⁷(py)₂ and tetracoordinate, distorted square planar for complexes supported by L⁸(py)₂. In addition to intense transitions between 200 and 300 nm, assigned as LMCT transitions, the complexes each exhibit a single ligand field transition between 600 and 650 nm. This d–d band exhibits a smooth hypsochromic shift as a function of increasing ligand size, occurring at 641, 623, and 601 nm for solutions of 4–6, respectively. This shift may be readily explained by consideration of the crystallographically defined structures of the complexes and the divergent amounts of overlap between ligand orbitals and the $d(x^2 - y^2)$ orbital of the central copper ion. From the perspective of crystal field theory, the $d(x^2 - y^2)$ orbital will be destabilized to the greatest extent when the basal plane interligand angles approach 90° (6; vide supra); significant angular deviations from 90° (as found in 4 and 5) will result in the $d(x^2 - y^2)$ orbital being stabilized relative to its energy in 6. As the d–d transition involves promotion of electrons into the $d(x^2 - y^2)$ orbital, the energy of this half-occupied orbital will be reflected directly in the energy of the optical transition.

The X-band EPR spectra of 1–3 in frozen CH₂Cl₂/CH₃CN (3:1 v/v) at 10 K are consistent with a tetragonal copper(II) environment. The nearly axial features (Table 3) have g_{\parallel} (2.21) > g_{\perp} (2.05) > 2.00 with A_{\parallel} of approximately 175×10^{-4} cm^{-1} , indicative of a $d(x^2 - y^2)$ ground state.¹⁷ The EPR features are entirely consistent with the geometric results deduced from the optical spectra.

Table 4. Electrochemical Data^a

complex	$E_{1/2}$ (mV) ^b	ΔE_p (mV) ^c	i_{pa}/i_{pc}
4	−650 ^d		
5	−196	63	0.84
6	−188	82	0.80
Cp ₂ Fe ^e	405	84	0.96

^a Data were collected in CH₃CN (0.1 M *n*-Bu₄NClO₄). See Experimental Section for complete details. ^b Quoted vs Ag/AgCl. ^c Measured at 100 mV/s. ^d Complex 4 was irreversibly reduced at this potential. ^e Ferrocene/ferrocenium couple; measured under identical experimental conditions.

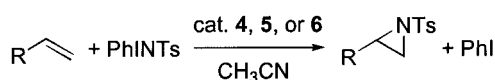
The divergent chelate ring sizes and the resulting copper ion geometries present in 4–6 may be expected to influence the Cu(II)/Cu(I) redox potentials in this series of compounds. Determination of these potentials is of interest because of the presumed involvement of redox chemistry (perhaps accessing the monovalent, divalent, and/or trivalent oxidation states of copper) in the copper-catalyzed aziridination of olefins by PhINTs. Thus, the redox potentials of 4–6 were determined in CH₃CN by cyclic voltammetry; the results of these studies are summarized in Table 4.

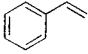
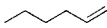
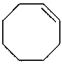
None of the copper(II) complexes exhibited significant redox behavior between 0 and 1.0 V vs Ag/AgCl, corresponding to the Cu(II)/Cu(I) redox couple. The cathodic behavior of these complexes varied, however, as a function of the supporting ligand. Complex 4 was irreversibly reduced in CH₃CN solution, which is not unexpected due to the rather rigid tetragonal geometry imposed by the tetradentate ligand L⁶(py)₂, which would destabilize the Cu(I) oxidation state. In contrast, complexes 5 and 6 exhibited quasi-reversible redox behavior at $E_{1/2} \cong -0.2$ V vs Ag/AgCl, redox potentials which are similar to that determined by Karlin and co-workers for [(TPA)Cu(CH₃CN)]⁺ [−0.19 V vs SCE; TPA = tris(pyridylmethyl)amine].¹⁸ The divergent redox behavior exhibited by 4–6 may be due, in part, to the increased flexibility of L⁷(py)₂ and L⁸(py)₂ relative to L⁶(py)₂. Thus, L⁷(py)₂ and L⁸(py)₂, which contain propylene bridges between tertiary amine donors, are able to undergo the small structural distortions necessary to provide a geometry favorable for Cu(I) (tetrahedral), while the less flexible chelate L⁶(py)₂ is not. Indeed, this flexibility is manifested in a ruffling of the equatorial plane in the solid-state structures of several

(17) Solomon, E. I.; Baldwin, M. J.; Lowery, M. D. *Chem. Rev.* **1992**, *92*, 521–542.

(18) Wei, N.; Murthy, N. N.; Chen, Q.; Zubieta, J.; Karlin, K. D. *Inorg. Chem.* **1994**, *33*, 1953–1965.

Scheme 3



Olefin ^a	Catalyst ^b	Yield, % ^c	Time, h
	4	85	8
	5	87	8
	6	80	8
	4	35	36
	5	0	24
	4	23	36
	5	0	24
	6	0	24

^a Approx. 20 eq. vs. PhINTs. ^b 5 mol % vs. PhINTs.

^c Isolated yield of N-tosylaziridine after purification.

complexes supported by L⁷(py)₂ and L⁸(py)₂, while the complexes supported by L⁶(py)₂ examined in this study were observed to contain unruffled equatorial planes.

Application to Catalytic Olefin Aziridination Reactions.

In a series of preliminary experiments designed to assess nitrene transfer reactivity, the structurally characterized copper(II) complexes **4–6** were examined for their ability to catalyze the aziridination of a series of olefins, including styrene, 1-hexene, and cyclooctene, using PhINTs as the nitrene source (Scheme 3). Complex **4**, supported by the relatively unhindered ligand L⁶(py)₂, demonstrated catalytic reactivity with the entire range of olefins examined, although the yields of aziridines derived from aliphatic olefins were significantly reduced relative to that obtained when styrene was used as the substrate. In contrast, while complexes **5** and **6** did catalyze the aziridination of styrene in good yields, these complexes, derived from the more hindered L⁷(py)₂ and L⁸(py)₂ ligands, failed to show any measurable reactivity with aliphatic olefin substrates. None of the catalysts functioned well at the low catalyst concentrations (0.5 mol % vs PhINTs) where the highly efficient copper catalyst [(*i*-Pr₃-TACN)Cu(O₂CCF₃)₂] operates.⁹ The extended time periods (8–36 h) required for completion of the aziridination reaction contrast with those observed for other copper catalysts^{3,9} and

suggest that some dynamic process (e.g., dissociation of an equatorial pyridine ligand) may be required to activate the (pre)-catalyst toward reactivity with PhINTs. Indeed, we have observed that copper complexes bearing labile, neutral donors in their equatorial positions catalyze nitrene transfer from PhINTs to olefins at significantly accelerated rates relative to those reported herein.¹⁹ While the steric properties of the supporting ligands L^{*n*}(py)₂ (*n* = 6–8) may influence the catalytic reactivity of **4–6**, the precise structural and electronic factors that govern the reactivity of these and other copper catalysts remain poorly defined and are the focus of current work in this laboratory.

Conclusion. We have described the syntheses and characterizations of a family of well-defined copper(II) complexes derived from new tetradentate ligands. All of the complexes function as catalysts in the aziridination of an activated olefin, styrene, by PhINTs; however, divergent reactivity is observed with less activated olefins. The results presented herein serve as a foundation for our continued efforts to rationally design efficient copper catalysts for the aziridination of structurally and electronically diverse olefins.

Acknowledgment. We thank the Camille and Henry Dreyfus Foundation (Faculty Start-Up Grant Program Award to J.A.H.), the donors of the Petroleum Research Fund, administered by the American Chemical Society (Grant 33450-GB3 to J.A.H.), the Research Corp. (Cottrell College Science Award to J.A.H.), and the University of Wisconsin—Eau Claire for financial support of this research. EPR studies at The University of Minnesota were supported by the National Institutes of Health (Grant GM-33162 to L.Q. and a predoctoral traineeship to M.P.M.).

Note Added in Proof. While this article was in press, we learned of an independent synthesis and structural characterization of L⁶(py)₂ and two complexes, [(L⁶(py)₂)Cu(ONO₂)]NO₃ and [(L⁶(py)₂)Cu₂(O₂CCH₃)₄], that are related to those described herein: Ratilainen, J.; Airola, K.; Frohlich, R.; Nieger, M.; Rissanen, K. *Polyhedron* **1999**, *18*, 2265–2273. We regret the omission of these compounds from the current discussion.

Supporting Information Available: X-ray crystallographic files, in CIF format, for **1–6** and EPR spectra of **1–3**. This material is available free of charge via the Internet at <http://pubs.acs.org>.

IC000664+

- (19) (a) Halfen, J. A. *Abstracts of Papers*, 219th National Meeting of the American Chemical Society, San Francisco, CA, 2000; American Chemical Society: Washington, DC, 2000: INOR 465. (b) Halfen, J. A.; Cea Plaza, M.; Hagen, C. M. To be submitted for publication.